A flexible eye-safe lidar instrument for elastic-backscatter and DIAL

Cite As: Robinson, I, Jack, J, Rae, C & Moncrieff, J 2012, 'A flexible eye-safe lidar instrument for elastic-backscatter and DIAL'. in *Proceedings of SPIE*. SPIE-The International Society for Optical Engineering, SPIE Remote Sensing 2012, Edinburgh, United Kingdom, 24-27 September.

DOI: 10.1117/12.974746

A flexible eye-safe lidar instrument for elastic-backscatter and DIAL

Proceedings of SPIE

Authors: Iain Robinson, Jim W. Jack, Cameron F. Rae, John Moncrieff

Address for correspondence:

John Moncrieff
School of Geosciences,
University of Edinburgh,
Crewe Building,
West Mains Road,
Edinburgh, UK
EH9 3JN

A flexible eye-safe lidar instrument for elastic-backscatter and DIAL

Iain Robinson[a], Jim W. Jack[a], Cameron F. Rae[b], John Moncrieff*[a]

[a]School of GeoSciences, University of Edinburgh, Crew Building, The King's Buildings, West Mains Road, Edinburgh, UK, EH9 3JN; [b]Photonics Innovation Centre, School of Physics and Astronomy, University of St Andrews, North Haugh, St Andrews, Fife, UK, KY16 9SS

ABSTRACT

Developments in lidar have been driven largely by improvements in two key technologies: lasers and detectors. We describe here a lidar instrument for atmospheric remote sensing using the elastic-backscatter and differential-absorption lidar (DIAL) techniques. The instrument features an all-solid-state laser source combined with a flexible approach to detection providing portability, eye-safe operation and high sensitivity.

The system is built around a custom-designed Newtonian telescope with a 0.38 m diameter primary mirror. Laser sources and detectors attach directly to the side of the telescope allowing for flexible customization with a range of equipment. The laser source is based on an optical parametric oscillator (OPO). The OPO is pumped by a neodymium-based diode-laser pumped solid-state laser and angle-tuned by rotating the nonlinear conversion crystal. This provides a wide range of available wavelengths suitable for lidar within the 1.55 μm to 3.10 μm spectral region, where there exists a relatively high exposure limit for eye safety. The OPO delivers 1 mJ output pulse energy which is expanded and then transmitted coaxially from the telescope. Our goal is to make vertically-resolved measurements of greenhouse gas concentrations using DIAL. The source can rapidly be tuned between the on-line and off-line wavelengths to make a DIAL measurement.

The use of the 1.6 μm wavelength region allows for several detection schemes. Whilst photodiode detectors are a very low-cost solution their limited sensitivity restricts the maximum range over which a signal can be detected. We therefore have designed the instrument to support alternative detection schemes including avalanche photodiodes (APDs).

Keywords: lidar, DIAL, photonics, OPO, greenhouse gases

1. INTRODUCTION

New instruments are needed to improve the quality and coverage of greenhouse gas measurements. Satellite-based sensors are the only instruments which give global coverage, however they generally provide column-weighted or column-integrated measurements[1] and have limited precision in the boundary layer, where evidence for sources and sinks of greenhouse gases reside. In contrast, ground-based measurements are the most reliable, but are limited in vertical range and resolution by the height of monitoring towers. Airborne instruments enable both high precision and vertical resolution, but are too costly for routine monitoring of a wide area.

Light detection and ranging (lidar) enables ground-based monitoring of the atmosphere with vertical resolution. Briefly, a lidar measurement is made by transmitting a laser pulse through the atmosphere, receiving the back-scattered light with a telescope and measuring the received power against the time elapsed since the pulse was transmitted (Δt). The distance from the lidar to the scattering, the range, can be calculated as $R = \frac{c\Delta t}{2}$ where c is the speed of light. The authoritative text on lidar by Measures[2] was first published in 1984. Since that date technological progress in photonics has made lidar less complex, improved instruments' performance and supported the development of new techniques.

For greenhouse gases, differential absorption lidar (DIAL) has become the favoured technique[3,4]. In DIAL, two laser pulses at different wavelengths are transmitted sequentially. One, the *on-line* wavelength is tuned to an absorption feature in the gas of interest, the other, the *off-line* is tuned slightly away (typically by ~0.2 nm) from the absorption wavelength. Comparison of the return signals at each wavelength allows calculation of the density of the gas as a function of range. The use of the off-line wavelength as a reference means that this calculation does not depend on any instrumental parameters, such as the receiver aperture area or the laser pulse duration.

* J.Moncrieff@ed.ac.uk; phone +44 131 650 5402

Remote Sensing of Clouds and the Atmosphere XVII; and Lidar Technologies, Techniques, and Measurements for Atmospheric Remote Sensing VIII, edited by E. I. Kassianov, A. Comeron, R. H. Picard, K. Schäfer, U. N. Singh, G. Pappalardo, Proc. of SPIE Vol. 8534, 85340X · © 2012 SPIE · CCC code: 0277-786/12/$18 · doi: 10.1117/12.974746

Eye-safety is a critical issue for any lidar. Instruments which are not eye-safe generate larger return signals due to the higher laser energies, however the ocular hazard greatly restricts the type of environments in which they can be used. Operation near airports or in urban areas is precluded. For a flexible, portable instrument it is therefore highly desirable that it be eye safe[5].

In this paper we report the initial measurements made with an instrument we are developing for DIAL. We outline the relevant background relating to scattering, discuss our choice of laser technology, describe the instrument in detail, and present our elastic-backscatter measurements.

2. BACKGROUND

The lidar equation is[6]

$$P(R) = \frac{KO(R)T(R)\beta(R)}{R^2} \tag{1}$$

where $P(R)$ is the received power from range R, K is a factor defined by the performance of the lidar system, $O(R)$ is the laser-beam receiver–field-of-view overlap function, $T(R)$ is the transmission factor for the path between the lidar and the range R and $\beta(R)$ is the backscattering coefficient at range R. The received power is inversely proportional to the square of the range as the scattering (generally) occurs isotropically and the area of the receiver aperture collects only a small fraction of the scattering sphere at range R.

The DIAL technique relies on transmitting a short pulse of laser radiation into the atmosphere where a small proportion of it is scattered by particulates in the path back into a sensitive receiver. The particulates include molecules and a wide range of small particles. Rayleigh scattering describes the elastic scattering of light by particles which are much smaller than the wavelength of the light, typically molecules, and is well-understood. The major contribution is from the molecules of nitrogen and oxygen in the atmosphere. The Rayleigh scattering cross section (σ) has been computed by several authors[7,8]. For air under standard conditions, and a wavelength of 1.5 μm, the tabulated cross section is $\sigma = 7.875\times10^{-29}$ cm^2. Using this value the fraction of a laser beam that is scattered into a lidar of given aperture and optical efficiency may be calculated[6], giving the received power for a given transmitted power. The results of this calculation using our instrument's parameters suggest that the received signal power at the detector from 1 km range will be 11 nW, reducing to 2.8 nW at 2 km due to the $\frac{1}{R^2}$-dependence. This sets a baseline requirement on the sensitivity and noise performance of the detector and its amplifier.

The Rayleigh scattering cross section is proportional to the inverse fourth power of the wavelength, so most Rayleigh scattering experiments are carried out in the ultraviolet spectral region. The Rayleigh scattering model breaks down when the particle size becomes larger than about 10 % of the wavelength of the incident radiation and this is the regime of Mie scattering. In the 1.5 μm region Rayleigh scattering is therefore expected to be very small and Mie scattering will dominate. The intensity and angular distribution of aerosol scattering depends strongly on the local aerosol composition and physical characteristics which vary widely with location and air quality. An important input is the aerosol size distribution and various approaches have been adopted[9,10]. However, for any specific observation, the aerosol characteristics may not be known and will be expected to be highly variable, especially in eastern Scotland where we made the measurements presented in this paper.

The laws that govern particulate scattering are complex and have only been derived for a limited number of particle characteristics. The characteristics which most determine the scattering are the particle size and the size distribution. A range of particle sizes is given by Measures[2] for a number of different types of atmospheres. Thus the value of $\beta(R)$ in Equation 1 will be difficult to predict with any useful accuracy and a flexible design is essential to allow adaptation to improve the performance where required. For this instrument, the features over which the designer has control have been optimized within the constraints of eye-safety, portability, simplicity and affordability. This approach has motivated us to adopt a coaxial geometry using the largest receiver aperture that is practically portable in a simple Newtonian optical configuration.

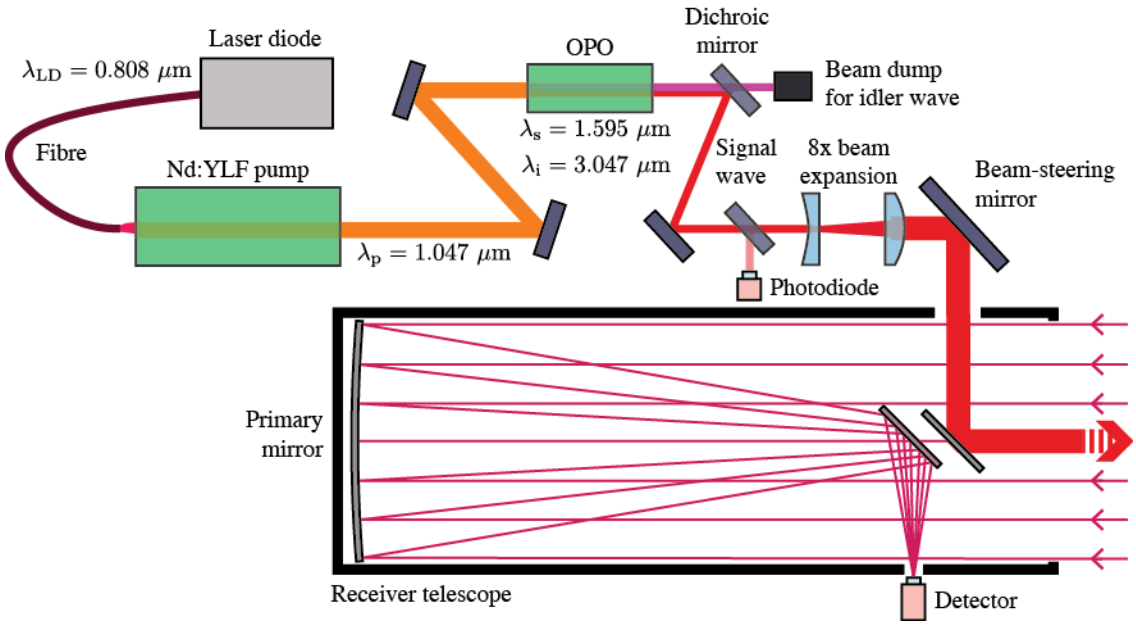

Figure 1. The lidar instrument. An optical parametric oscillator (OPO) is pumped by a diode-pumped neodymium-doped yttrium lithium fluoride (Nd:YLF) laser. The wavelengths of the laser diode (λ_{LD}), Nd:YLF pump laser (λ_p), and the OPO signal (λ_s) and idler (λ_i) waves are shown. A photodiode is used to provide a power and timing reference. The OPO signal wave is separated from idler, expanded, and transmitted along the axis of the receiver telescope. The received signal is focused by the telescope into the detector.

3. THE LIDAR INSTRUMENT

3.1 Choice of laser technology

The key consideration for an eye-safe instrument is the wavelength of the transmitter. The visible–near-infrared region 0.4–1.4 µm should be avoided as these wavelengths are easily transmitted through the human cornea and therefore present a significant eye hazard. The maximum permissible exposure (MPE)[11] in this region is therefore low. Outwith this region, the MPE is substantially more favourable, allowing the use of much higher pulse energies. The wavelength region near 1.6 µm, the telecom window, is particularly attractive for lidar as a wealth of telecommunications technologies can be applied and low-cost high-sensitivity detectors, such as avalanche photodiodes[12], are available.

The ideal laser source for DIAL would be rapidly tunable between the on-line and off-line wavelengths, have narrow spectral line-width to match the absorption feature in the gas, have a low divergence, and provide a laser pulse energy and average power close to the MPE. Several types of laser have been applied to meet these demands. Stimulated Raman scattering in high-pressure methane has been used[5,13] to convert the fundamental wavelength of an Nd:YAG laser (1.064 µm) to the more eye-safe 1.54 µm. However, solid-state devices are preferable for field use as they avoid the need to handle methane and are not limited in wavelength tuning by the Raman spectrum of the gas. We chose to use an optical parametric oscillator (OPO) as this is an established solid-state technology that is capable of reliable operation, whilst providing the precision wavelength tuning required for DIAL. OPOs have been used for several DIAL systems operating in the telecom window near 1.6 µm[4,14].

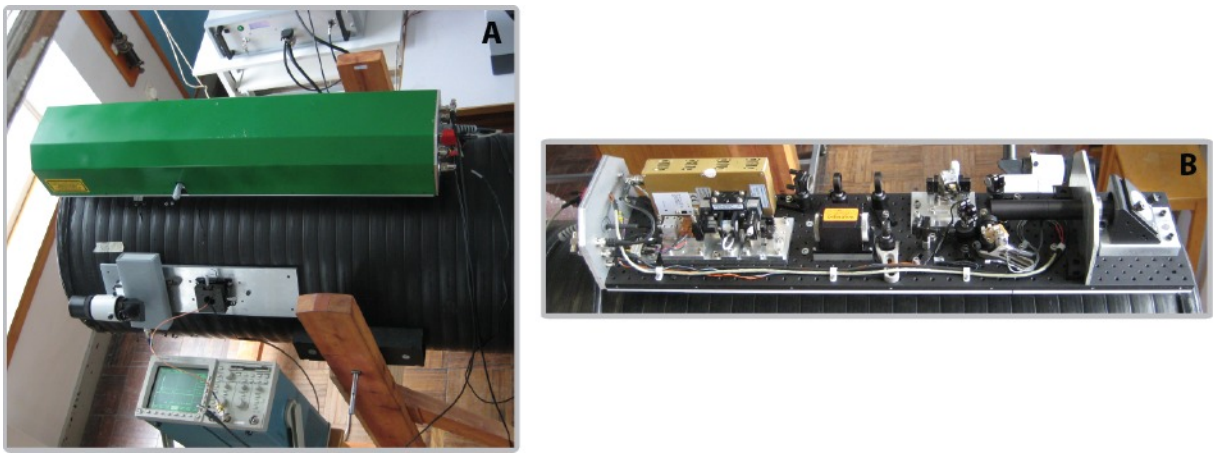

Figure 2. A photograph of the complete instrument (A) and an internal photograph (taken from the opposite side) of the laser (B).

3.2 Transmitter

A diagram of the instrument is shown in Figure 1. The OPO is pumped by a neodymium-doped yttrium lithium fluoride (Nd:YLF) laser. The Nd:YLF laser is Q-switched and provides an output energy of 4.5 mJ per pulse at a repetition rate of 50 Hz and a wavelength of 1.047 µm. The OPO uses a type II critically phase-matched potassium titanyl phosphate (KTP) nonlinear crystal to convert the pump wavelength to 1.595 µm (signal) and 3.047 µm (idler). The wavelengths can be fine-tuned by rotating the crystal. The useful output conversion efficiency was measured as 21 %, with 0.76 mJ in the signal wave and 0.20 mJ in the idler, although this could be improved with the use of more optimal optical coatings as the overall down-conversion efficiency was measured through pump depletion to be close to 35 %. The pulse duration (full width at half maximum) was measured with a fast photodiode as 4.6 ns. The signal wavelength is used as the transmitter. A dichroic mirror separates it from the (unused) idler. A small portion of the transmit beam is picked off into a photodiode to monitor the transmitted pulse energy and provided a zero time ($\Delta t = 0$) reference signal.

The transmit beam is expanded with a 8x Galilean lens pair. This expansion serves dual purposes. Firstly, since the OPO output is above the MPE, it reduces the irradiance and the radiant exposure, rendering the transmit beam eye-safe. Secondly, it reduces the output divergence to an angle within the receiver telescope's field-of-view. The ($\frac{1}{e^2}$, full angle) divergence of the OPO signal output was measured as 5.1 mrad. The expansion reduces this by a factor of 8, to 0.6 mrad. The transmit beam ($\frac{1}{e^2}$) diameter leaving the instrument was measured as 9.3 mm. If required the beam could be expanded further, up to the size of the telescope secondary mirror (90 mm).

3.3 Receiver

The receiver is based around a Newtonian telescope with an aperture diameter of 380 mm, and a focal length (f) of 1150 mm. The focal ratio is f/3.03. The laser and the detector attach directly to the telescope tube as shown in the photograph in Figure 2. The telescope focuses the return signal onto the detector, an indium gallium arsenide (InGaAs) PIN photodiode (G8370-01, Hamamatsu). The photodiode has an active area of 1 mm diameter (D), a cut-off frequency of 35 MHz and a sensitivity of 0.95 A/W.

The receiver field-of-view (full) angle is given by $\frac{D}{f}$ where D is the photodiode diameter (1 mm) and f is the focal length of the primary mirror (1150 mm). The field-of-view is therefore 0.9 mrad. As this is greater than the laser divergence (0.6 mrad after expansion) the transmitted beam lies completely within the receiver's field-of-view.

The photodiode signal is amplified with a custom-built transimpedance amplifier. Although uncalibrated, the detector response to incident light can be estimated by multiplying the amplifier gain, 3.5×10^6 V/A, by the specified photodiode sensitivity (0.95 A/W) to give 3.3 V/µW. The cut-off frequency (f_c) of the amplifier was calculated as 10 MHz. As this

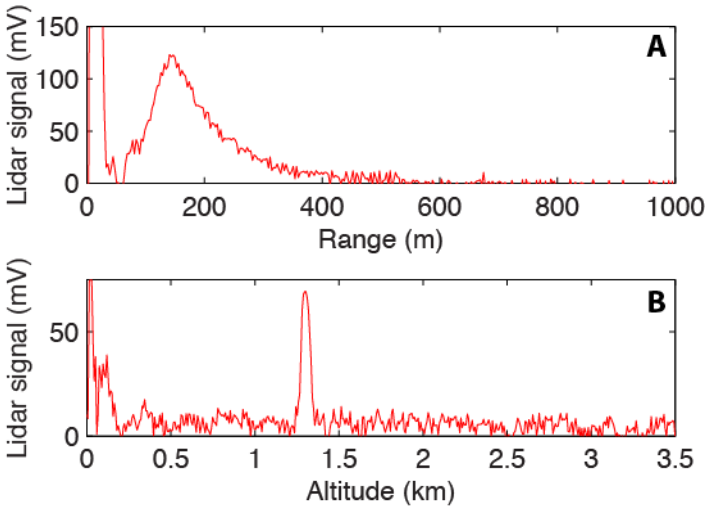

Figure 3. Lidar return signals over a short range of 1 km (A), and a longer range of 3.5 km (B). Signal (A) shows the outgoing pulse as it leaves the transmitter near 0 m, followed by a peak due to atmospheric scattering which is centred at 140 m. Signal (B) shows a return from a cloud at an altitude of 1.3 km.

frequency is lower than that of the photodiode (35 MHz), it is the amplifier bandwidth which determines the range resolution. The rise time is calculated as $\frac{0.35}{f_c}$=36 ns, giving a range resolution of 5 m.

The lidar signal was digitzed with an oscilloscope. It was averaged over 256 traces to reduce the effect of random noise on the signal. The traces were transferred to a computer over a serial cable at a maximum rate of 3 s/trace.

4. LIDAR MEASUREMENTS

4.1 Results

To evaluate the instrument a number of measurements of the elastic-backscatter lidar signal were made. All the signals were recorded in St Andrews, Scotland.

Figure 3(A) shows a typical return signal recorded over a range from 0 to 1 km. The zero range reference (R=0 m) is taken from a photodiode inside the laser (shown in Figure 1). The signal is the average of 256 traces. The large peak immediately after zero range (and beyond the upper limit of the graph) is due to the detector picking up the outgoing transmitted pulse, probably from scatter inside the telescope. The broad peak centred on 140 m is likely to be a combination of Rayleigh and Mie scattering, although it is difficult to determine the expected received power from Mie scattering without knowledge of the local atmospheric aerosol composition. The position of the peak is due to the combination of two effects. The overlap function, $O(R)$ in Equation 1, represents the fraction of the area illuminated by the transmitted beam which can be "seen" by the receiver telescope. At zero range the receiver cannot detect the transmitted pulse as it is obscured by the secondary mirror. As the range increases the pulse moves out of the shadow of the secondary mirror increasing the received signal power[6]. At the same time, the received power from scattering reduces with range, due to the $\frac{1}{R^2}$ term in Equation 1, causing the falling edge of the peak. It was found that the position and height of this peak changed if the instrument was deliberately misaligned, as this moved the transmit beam moved out of the obscuration.

Figure 3(B) shows a separate lidar signal recorded from 0 to 3.5 km. In order to measure the vertical range (altitude) the instrument was directed upwards by positioning a 600 mm wide flat folding mirror angled at 45° in front of the telescope. The signal shows strong scattering from a cloud at an altitude of 1.3 km.

In order to evaluate the maximum range of the lidar, signals were also recorded with the instrument pointed at an elevation of 8° to the horizontal. Figure 4 shows the return signal from cloud at 5.5 km. This gives an estimate of the maximum range at which the lidar can detect a return signal above the noise level of the detector.

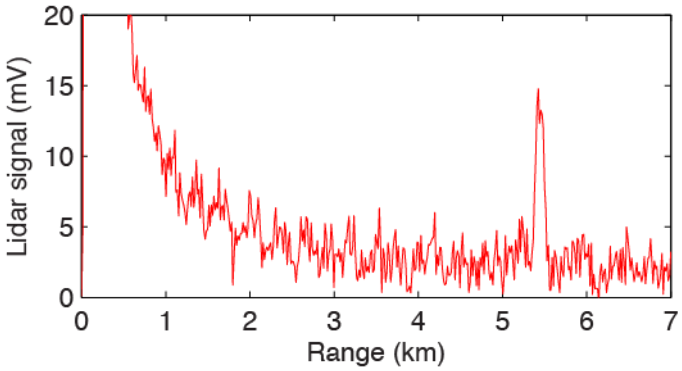

Figure 4. The lidar signal measured with the instrument pointed at an elevation of 8° to the horizontal. The return signal from a cloud at 5.5 km gives an estimate of the maximum range of the instrument.

The dynamic nature of the return signals from cloud can be observed by recording multiple traces as a time series. With the lidar directed vertically (from the folding mirror) series of return signals were recorded over time. The cloud altitude over time was determined by finding the altitude of the peak in each trace above a threshold set to the noise level of the detector. The first kilometre (R=0–1 km) was excluded from the analysis as this range contains both the outgoing transmit pulse and the atmospheric scattering peak. The results of this analysis are shown in Figure 5 for two series of lidar signals recorded over 10 min intervals on consecutive days. Figure 5(A) was recorded on an overcast day and shows a near-constant cloud-base altitude. The abrupt shift in cloud altitude from 1.7 km to 2.3 km at 7 min is likely due to a separate cloud drifting into the instrument's field-of-view. Figure 5(B) was recorded on a clear, windy day and shows scattered cloud drifting above the instrument.

An automated report from a nearby air defence station (RAF Leuchars) made 30 min after recording the signal in Figure 5(A) indicated few clouds at 0.8 km, broken cloud at 1.5 km and overcast cloud at 2.4 km. This is consistent with the measured 2.3 km constant cloud altitude from 7 min onwards. Similarly, a report made 2 min after recording the signal in Figure 5(B) indicated few clouds 1.2 km, consistent with the intermittent cloud seen around 1.4 km.

4.2 Discussion

These results demonstrate the operation of the instrument for detection of signals due to elastic back-scatter. A broad peak due to Rayleigh or Mie scattering could be detected, however the range of this detection was limited by the detector signal-to-noise. Strong scattering signals from cloud were detected and these signals have a form consistent with reports in the literature[10,15]. The furthest detectable cloud signal was found to be 5.5 km (Figure 4). The signal-to-noise ratio of this peak is around 7, suggesting that signals from further ranges would be obscured by detector noise.

To improve the instrument's overall sensitivity it is our intention to replace our current photodiode detector with an avalanche photodiode (APD). The internal gain in an APD will provide an improved signal-to-noise ratio[16], extending the maximum range and allowing detection of the scattering peak to greater ranges. In combination with further developments of our laser system this will enable us to make DIAL measurements.

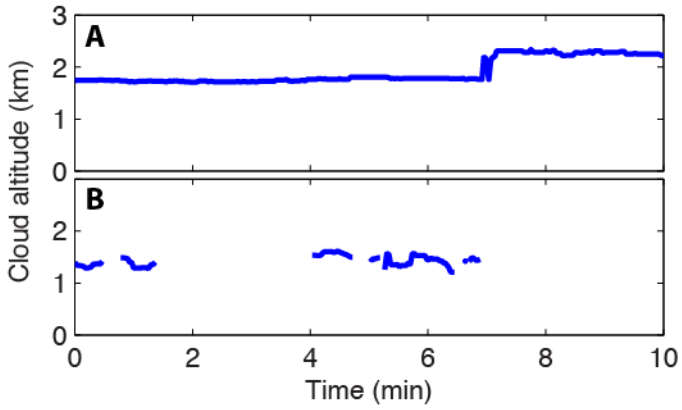

Figure 5. Cloud altitude over two 10 min periods on different days. Graph (A) shows a constant cloud base on a calm day with an abrupt change in altitude around 7 min. Graph (B) shows scattered clouds passing above the instrument on a windy day.

5. CONCLUSION

We have demonstrated the operation of an eye-safe lidar instrument at a wavelength of 1.6 μm based on an optical parametric oscillator laser source, a 0.38 m diameter receiver telescope and a photodiode detector. The elastic-backscatter from the atmosphere was detected over short ranges, and the return signal from cloud at ranges up to 5.5 km. The instrument will serve as a platform for our development of a DIAL lidar.

ACKNOWLEDGEMENTS

This work was partly funded by The University of Edinburgh under a Development Grant with support from an EU FP7 programme "InGOS - Non CO_2 GHG Balance of Europe (INFRA-2011-1.1.11)"

REFERENCES

[1] Bréon, F.-M. and Ciais, P., "Spaceborne remote sensing of greenhouse gas concentrations," Comptes Rendus Geoscience 342(4–5), 412–424 (2010). doi:10.1016/j.crte.2009.09.012

[2] Measures, R. M., [Laser Remote Sensing: Fundamentals and Applications], Krieger Publishing Company (1992).

[3] Gibert, F., Flamant, P. H., Cuesta, J. and Bruneau, D., "Vertical 2-μm heterodyne differential absorption lidar measurements of mean CO_2 mixing ratio in the troposphere," J. Atmos. Oceanic Technol. 25(9), 1477–1497 (2008). doi:10.1175/2008JTECHA1070.1

[4] Sakaizawa, D., Nagasawa, C., Nagai, T., Abo, M., Shibata, Y., Nakazato, M., Sakai, T., "Development of a 1.6 μm differential absorption lidar with a quasi-phase-matching optical parametric oscillator and photon-counting detector for the vertical CO_2 profile," Appl. Opt. 48(4), 748–757 (2009). doi: 10.1364/AO.48.000748

[5] Mayor, S. and Spuler, S. M., "Raman-shifted eye-safe aerosol lidar," Appl. Opt. 43(19), 3915–3924 (2004). doi:10.1364/AO.43.003915

[6] Wandinger, U., "Introduction to lidar," in Weitkamp, C. (ed.), [Lidar: Range-Resolved Optical Remote Sensing of the Atmosphere], Springer, Berlin and Heidelberg, 1–18 (2005). doi:10.1007/b106786

[7] Bucholtz, A., "Rayleigh-scattering calculations for the terrestrial atmosphere," Appl. Opt. 34(15), 2765–2773 (1995). doi:10.1364/AO.34.002765

[8] Penndorf, R., "Tables of the refractive index for standard air and the Rayleigh scattering coefficient for the spectral region between 0.2 and 20.0 μm and their application to atmospheric optics," JOSA 47(2), 176–182 (1957). doi:10.1364/JOSA.47.000176

[9] Prilutsky, O. F. and Fomenkova, M. N., "Laser beam scattering in the atmosphere," Science & Global Security: The Technical Basis for Arms Control, Disarmament, and Nonproliferation Initiatives 2(1), 79–86 (1990). doi: 10.1080/08929889008426349

[10] Werner, C., Streicher, J., Leike, I. and Münkel, C., "Visibility and cloud lidar," in Weitkamp, C. (ed.), [Lidar: Range-Resolved Optical Remote Sensing of the Atmosphere], Springer, Berlin and Heidelberg, 1–18 (2005). doi:10.1007/b106786

[11] British Standards Institute, "Safety of laser products," BS EN 60825-1:2007 (2007).

[12] Maruyama, T., Narusawa, F., Kudo, M., Tanaka, M., Saito, Y., and Nomura, A., "Development of a near-infrared photon-counting system using an InGaAs avalanche photodiode," Opt. Eng. 41(2), 395–402 (2002). doi:10.1117/1.1431556

[13] Patterson, E., Roberts, D., and Gimmestad, G., "Initial measurements using a 1.54-μm eyesafe raman shifted lidar," Appl. Opt. *28*(23), 4978–4981, (1989). doi:10.1364/AO.28.004978

[14] Amediek, A., Fix, A., Wirth, M., and Ehret, G., "Development of an OPO system at 1.57 μm for integrated path DIAL measurement of atmospheric carbon dioxide," Appl. Phys. B 92(2), 295–302, (2008). doi:10.1117/1.1431556

[15] Lavrov, A., Utkin, A. B. and Vilar, R., "Simple eye-safe lidar for cloud height measurement and small forest fire detection," Opt. Spectrosc. 109(1), 144–150 (2010). doi:10.1134/S0030400X10070246